J. Fluid Mech. (1971), *vol.* 48, *part* 2, *pp.* 353–364
Printed in Great Britain

Sting-free drag measurements on ellipsoidal cylinders at transition Reynolds numbers

By M. JUDD,† M. VLAJINAC AND E. E. COVERT

Massachusetts Institute of Technology, Department of Aeronautics and Astronautics, Aerophysics Laboratory, Cambridge, Massachusetts

(Received 12 August 1970)

The drag coefficient for a family of axially symmetric ellipses of fineness ratio 4, 5 and 8 was measured using magnetically suspended models. The Reynolds number ranged up to 10^6. Thus, only the blockage interference is present, which may be partially allowed for by classical wind tunnel procedures. It is expected that the drag values presented here are accurate to 1 %.

1. Introduction

Theoreticians find ellipsoids of revolution and their limiting case, spheres, attractive models for studying the characteristics of low speed flows. They are able to solve the basic equations by separation of variables in a straightforward way. The resulting pressure distributions tend to be in reasonably good agreement with experimental results near the forward stagnation point. However, the effects of viscosity are such that the predicted pressures are rarely measured well downstream on these bodies. Further, separation is hard to predict so estimates of the drag coefficient are often seriously in error. The advent of the high speed computing machines offers a possibility of finding numerical solutions that include the effects of viscosity. Ellipsoids of revolution are still attractive for this purpose because their surfaces possess continuous curvature.

The drag coefficient of these ellipsoidal shapes is also difficult to obtain experimentally. Wind tunnel measurements are usually subject to a certain amount of error caused by interference between the support and the model. It is difficult to obtain drag data from flight testing since many simple bodies are unstable. Some free flight tests have been made of spheres for which the stability is not of great importance. These flight tests are possible if the sphere is dense enough that its trajectory is straight.‡ The drag data reported here were obtained by suspending ellipsoidal models in a subsonic wind tunnel by means of a magnetic balance and suspension system§ (Stephens 1969). In this way, the support

† Present address: Department of Aeronautics and Astronautics, The University of Southampton, Southampton SO9 5NH, England.

‡ The problem of obtaining a straight trajectory may be illustrated by the following elementary experiment. In dropping a small sphere into a tall cylinder filled with dense fluid, the motion of the sphere tends to an irregular helix as it falls to the bottom of the container.

§ The authors would like to thank Mr Fred Daum of the Aerospace Research Laboratories for permission to use equipment developed under a contract AF 33 (615)-1470.

interference is non-existent. For the same Reynolds number and surface condition, the difference between the wind tunnel drag and (hypothetical) free flight drag lies in the wall interference effect. For these experiments, this latter effect was qualitatively evaluated by testing three geometrically similar models varying in blockage from about 0·3 % to 3 %. The wind tunnel interference effects were determined by cross plotting the measured drag coefficient, at constant Reynolds number, against model size. The corrected data provides a reliable value for the drag coefficient in the length Reynolds number range 2×10^5 to 10^6. This is a range in which transition occurs. Accuracy of shape, surface condition and tunnel wall interference may all have an influence on transition and separation characteristics. No symmetric study was undertaken of drag sensitivity to shape nor was the boundary layer artificially tripped except in one case. All the models had a similar smooth finish although not highly polished.

2. Description of experiment

The experiment was performed in the 7 in. × 7 in. octagonal Eiffel type wind tunnel at the M.I.T. Aerophysics Laboratory. This wind tunnel was a continuous speed control from a Mach number of essentially 0 to 0·5. All of the experiments reported here were conducted at Mach numbers low enough that compressibility effects could be assumed negligible. The tunnel itself was designed to have low turbulence flows, which was verified during tunnel calibration (Vlajinac 1970).

	Ellipsoids of revolution							
Model	L	D	$\frac{1}{4}\pi D^2$			Blockage	Solid blockage	
L/D	(Dimensions in inches)			T_0 °C	P_{ATM} in. Hg	(%)	factor ϵ_s	Figure
8	3·00	0·375	0·1104	25·0	30·23	0·3	0·0034	4(*a*)
8	6·00	0·750	0·4418	26·3	29·88	1·3	0·0136	4(*b*)
8	9·00	1·125	0·9940	25·6	30·22	3·0	0·0300	4(*c*)
4	4·00	1·00	0·7854	26·3	30·23	2·4	0·0100	4(*d*)
5	4·00	0·800	0·5027	26·2	30·23	1·5	0·0068	4(*e*)

Humidity unknown, probably around 60 % ± 20 %.

TABLE 1. Test conditions

Additional information regarding the wind tunnel turbulence level and velocity uniformity is given in appendix A.

In operation the model was suspended in the centre of the test section. Its position was monitored with the aid of two surveying transits to ensure that the absolute position was fixed to a thousandth of an inch.

The test conditions are shown in table 1. The room temperature and the pressure in the test room were recorded throughout a run, and were found to be constant over that time interval. The static pressures from the two speed setting holes in the tunnel contraction section were fed to a diaphragm-type electrical

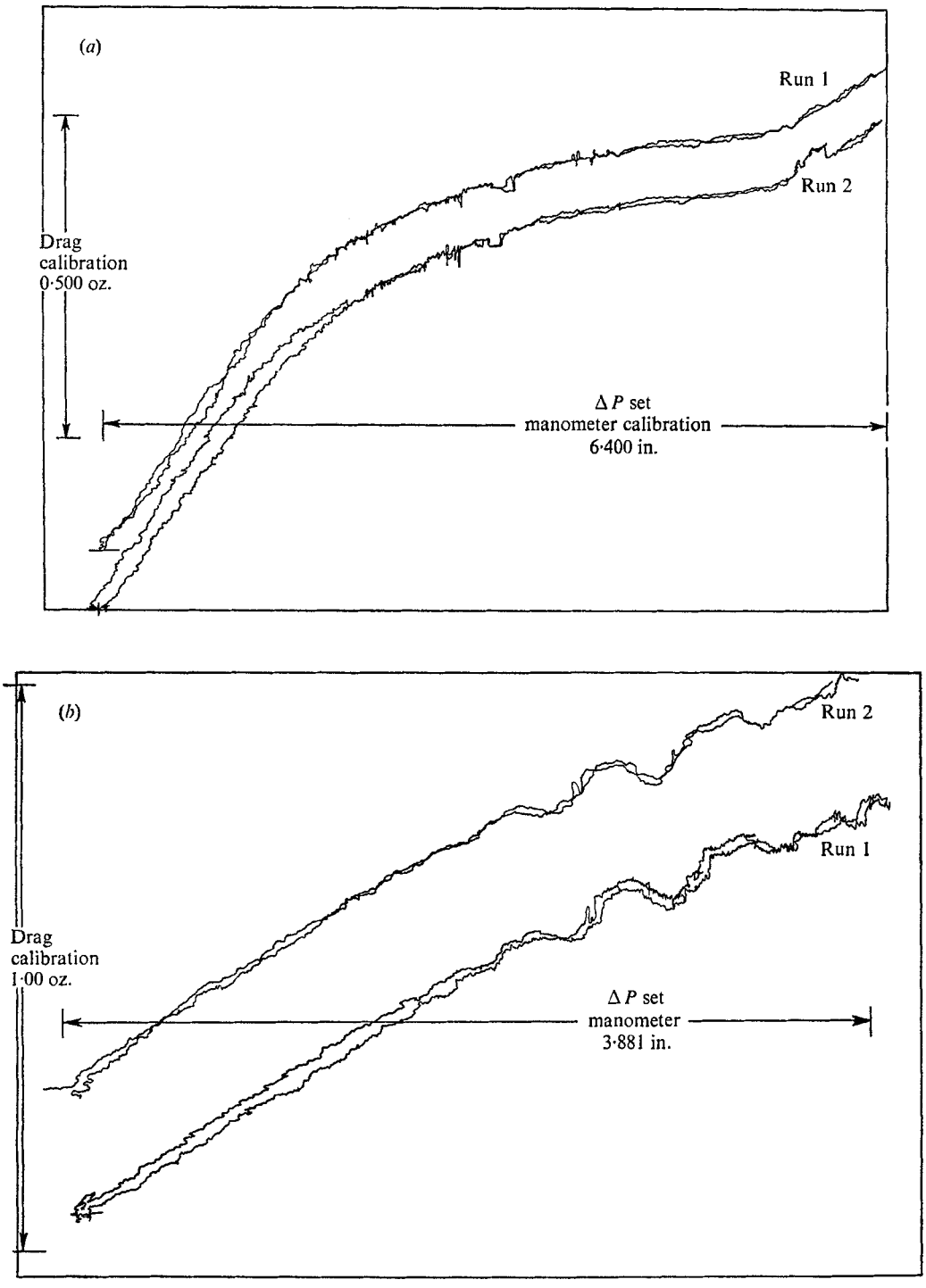

FIGURE 1. Raw data. Model: ellipsoid of revolution $L = 4$ in., $L/D = 4$.
(*a*) Temperature = 26·3° C, pressure = 30·23 in. Hg.
(*b*) Temperature = 25·6° C, pressure = 30·22 in. Hg.

transducer.† The output of this transducer drove the abscissa of a 12 in. X–Y plotter. The drag current was used to drive the ordinate of the same plotter. Thus drag was recorded as a continuous function of the dynamic pressure. A run consisted of locating the model in the test section, gradually increasing the tunnel speed and then gradually decreasing the tunnel speed. The rate of increase and decrease selected was such that the raw data of the model drag was essentially coincident in both the up and the downward velocity change, thus in effect providing steady state data. Figure 1 shows a typical raw data curve of drag *vs.* dynamic

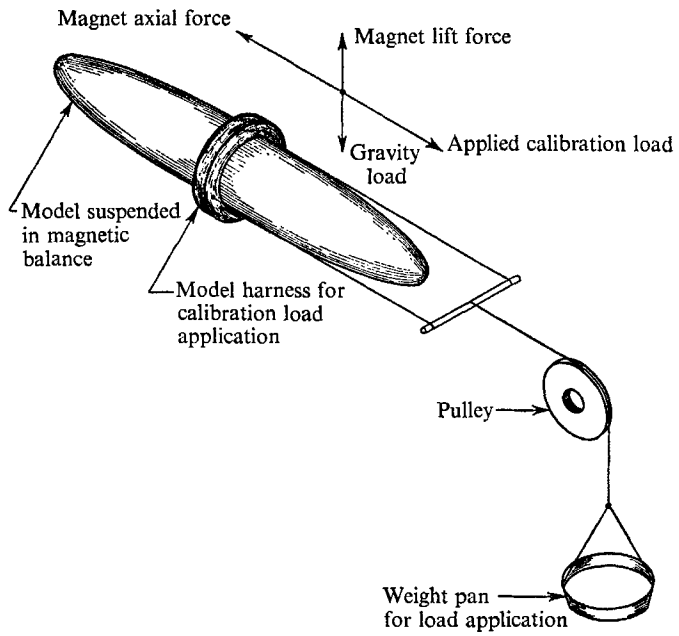

FIGURE 2. Sketch showing calibration method. In wind tunnel: magnetic axial force is equal and opposite to aerodynamic drag on model. During calibration: magnetic axial force is equal and opposite to applied calibration load on model.

pressure. Repeat runs were recorded by shifting the initial location of the pen.‡ A particular model was calibrated before and after each run by the following procedure. The model was located in the wind tunnel at the same position as it was during the wind tunnel run. A harness attached to the model with a string leading around a pulley to a weight pan (see figure 2) allowed a desired load to be applied during the force calibration. A total of 0·25 oz. was added and the pen travel noted as shown in figure 1. Figure 3, from Vlajinac & Gilliam (1970), indicates that this simple calibration and linear interpolation is accurate to 0·3%. The weight, plus pan, plus string, was assumed to be equal to the horizontal force acting on the model.

† The difference between these two pressures is proportional to the dynamic pressure in the test section (Vlajinac 1970).

‡ In preparation of this note, it was found that this procedure introduced a systematic bias into the data. No attempt was made to correct for this bias.

It can be shown that the magnetization level of the elliptical models, which were constructed of 99·9 % pure iron, is to the first order a function of the demagnetization factor, rather than due to the permeability of the material (Bozorth 1951).† Consequently, the calibration is temperature independent.

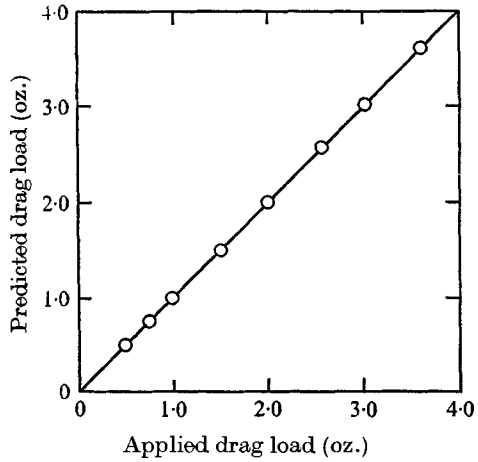

FIGURE 3. Comparison of calibrated drag *vs.* applied drag (from figure A-1 of Vlajinac & Gilliam 1970). Maximum deviation 0·3 %.

$Re \times 10^{-5}$	2·09	5·03	7·01	10·11
$L = 3$ in.: C_D	0·0867 ± 0	0·0644 ± 0·0008	0·0613 ± 0·0009	—
$L = 6$ in.: C_D	—	0·0615 ± 0·001	0·0596 ± 0·0002	0·0588 ± 0·0008
$L = 9$ in.: C_D	—	0·0661 ± 0	0·0632 ± 0·0020	0·0593 ± 0·0002

Based on a minimum of 3 points.

TABLE 2. Repeatability of drag coefficient 8:1 ellipse

The calibration factor for the dynamic pressure was found to be accurate to within a quarter of a per cent. The measured distances on the chart are accurate to 0·05 in. The effect of the machining errors on the model of two one-thousands of an inch, and the ability to read current to one part in a thousand may be combined to give an estimated accuracy of the drag coefficient of plus and minus 0·9 %. Table 2 shows repeatability at several Reynolds numbers based upon a minimum of 3 runs (Josephs & Brook 1953). The scatter varies from 0 to 3 %. The average is about 0·9 % and is thus consistent with the estimate of error.

3. Analysis of data

Figures 4(*a*)–(*e*) show plots of the drag coefficient as a function of Reynolds number for runs listed in table 1. The data plotted on figures 4(*a*)–(*e*) are discrete values picked off the continuous chart plots.

† The correction series are in powers of the product of magnetic permeability and the demagnetizing factor. In this case, the product is less than 10^{-3}.

The raw data for the 8:1 ellipse was first analyzed to determine the effect of the model size in terms of the wind tunnel blockage. Figures 4(*a*)–(*c*) were cross-plotted at constant Reynolds numbers as shown in figure 5. The theoretical variation of the tunnel drag coefficient (Pankhurst & Holder 1952, pp. 341–2) with the solid blockage factor ϵ_s is also shown in figure 5. The definition and application of the factor ϵ_s is summarized in appendix B. In comparison with the data, the theory is qualitatively correct, but there are differences in detail. The theoretical correction was applied to all the data and the collapse is shown in figure 6. The results in figure 6 were measured from models with a smooth surface and an essentially laminar boundary layer. A mean of these results is presented in

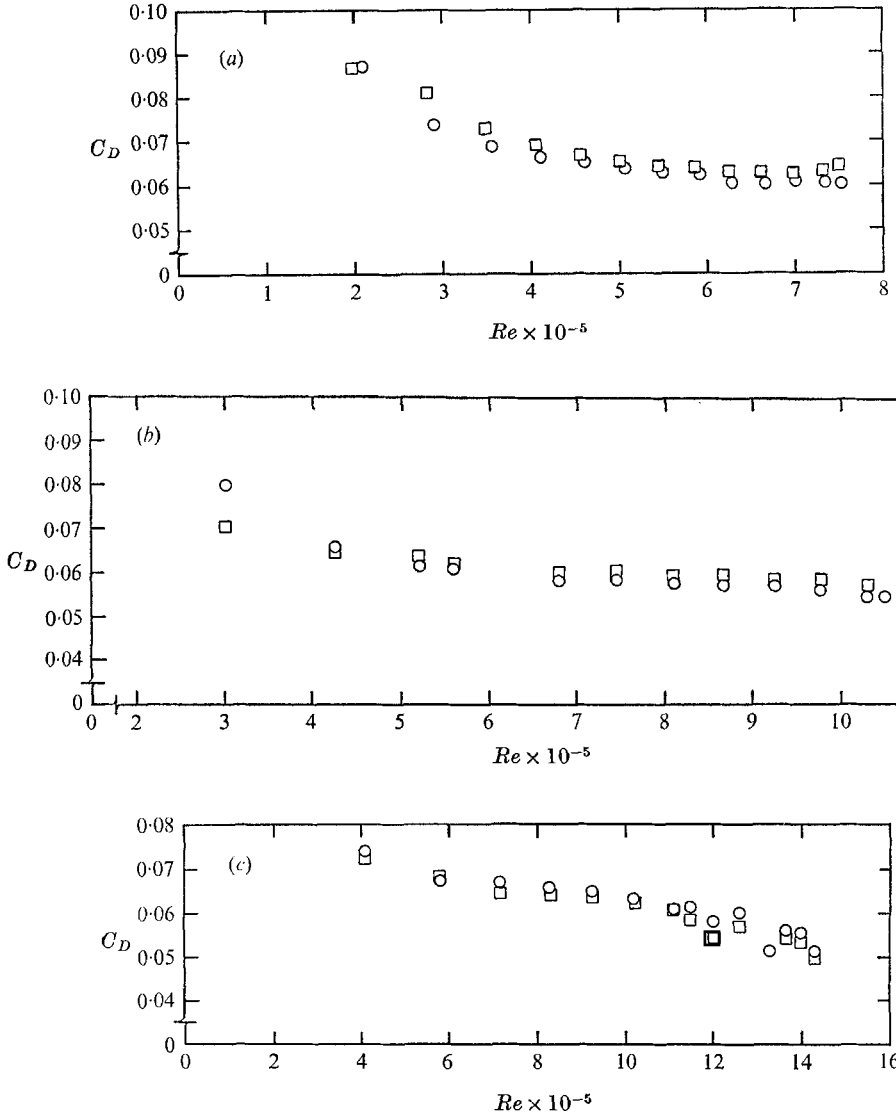

FIGURE 4(*a*), (*b*), (*c*). For legend see opposite page.

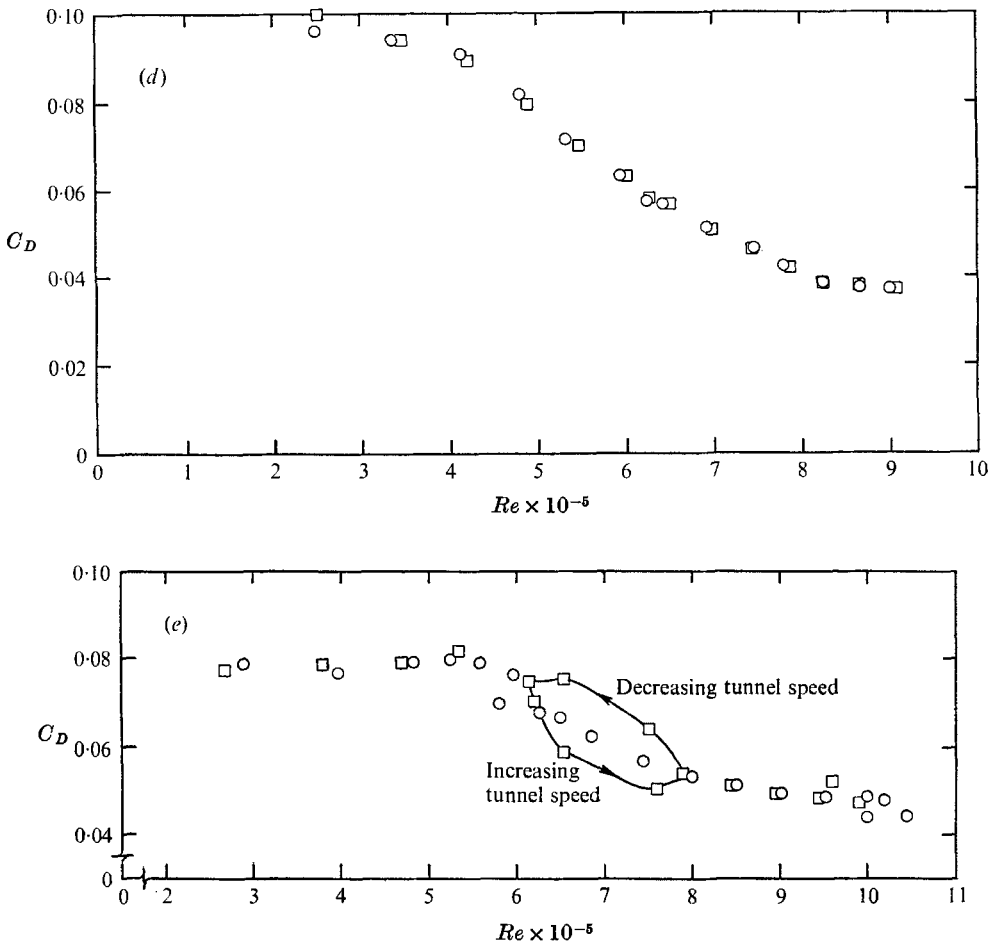

FIGURE 4. C_D versus Re. ○, run 1; □, run 2. (*a*) 8:1 ellipsoid 3 in. long; (*b*) 8:1 ellipsoid 6 in. long; (*c*) 8:1 ellipsoid 9 in. long; (*d*) 4:1 ellipsoid 4 in. long; (*e*) 5:1 ellipsoid 4 in. long.

figure 7 for comparison with theoretical drag predictions for laminar and turbulent boundary layers. Also included are results obtained for a 6-inch long ellipsoid fitted with a boundary-layer trip. The trip consisted of a single loop of wire 0·0055 in. in diameter fixed axisymmetrically at a distance 1·375 in. from the nose. The theoretical curves were obtained by assuming two-dimensional boundary-layer growth and no separation.

The data for the 4:1 and 5:1 ellipsoids were corrected for blockage and are shown in figure 8 for comparison with the 8:1 results.

Initially it seemed desirable to provide a more accurate comparison of the estimated and measured drag. The inviscid pressure distribution can be computed (Durand 1943) in terms of the tangential velocity.† The velocity distribution can also be used to compute the shear distribution in laminar flow

† The solution for the potential flow about an ovary ellipsoid of revolution is available in Lamb (1932), Batchelor (1967), or a number of other sources.

(Rosenhead 1963, pp. 431–2) and the separation point (Curle & Skan 1957). The latter is not well defined in axially symmetric flow. Further, an estimate of the drag needs an assumption about the static pressure distribution downstream of the separation point. Since the data seem to be located primarily in the transition régime from laminar to turbulent boundary layer, and because of the uncertainty about the separation point, these detailed calculations were not made.

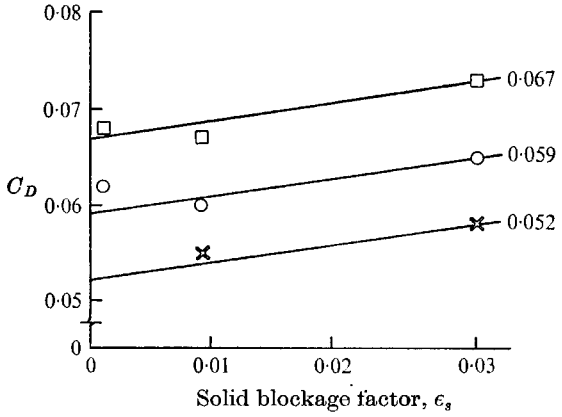

FIGURE 5. Effect of solid blockage on C_D. Reynolds number: ⊠, 12×10^5; ○, 8×10^5; □, 4×10^5. ——, theory.

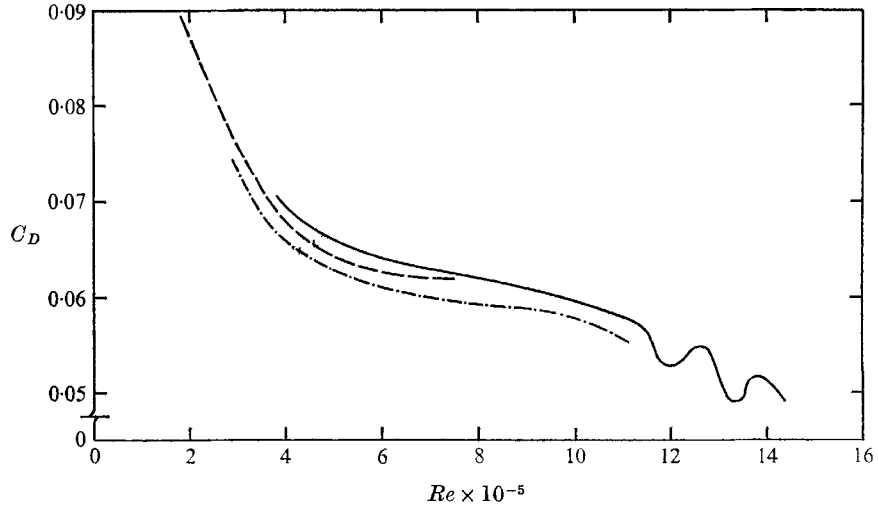

FIGURE 6. C_D versus Re corrected for blockage, 8:1 ellipsoid. Length in.: — — —, 3; –·–, 6; ——, 9.

4. Discussion

The collapse of the data in figure 6 on the basis of length Reynolds number indicates that the tunnel flow and model surface conditions produce essentially the same laminar boundary-layer state on all three models. This is confirmed

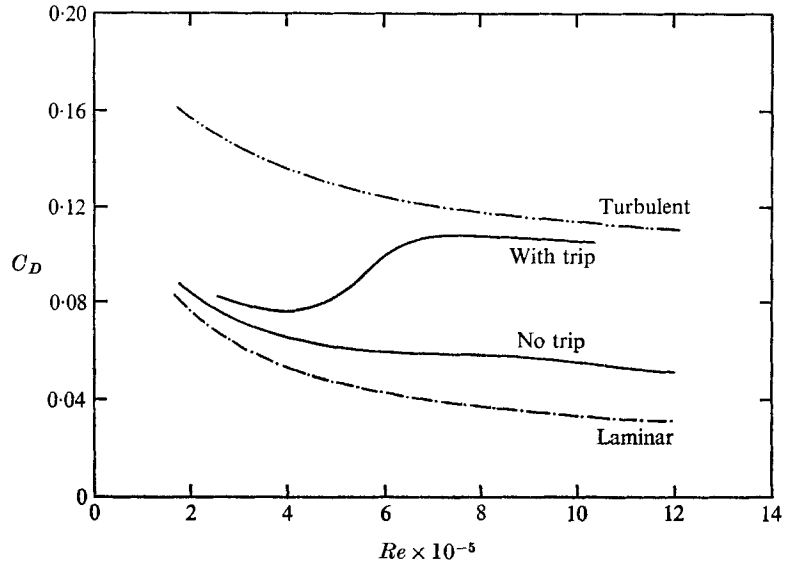

FIGURE 7. C_D versus Re, comparison with two-dimensional boundary-layer theory. ——, measured; —··—, —·—, two-dimensional boundary-layer theory.

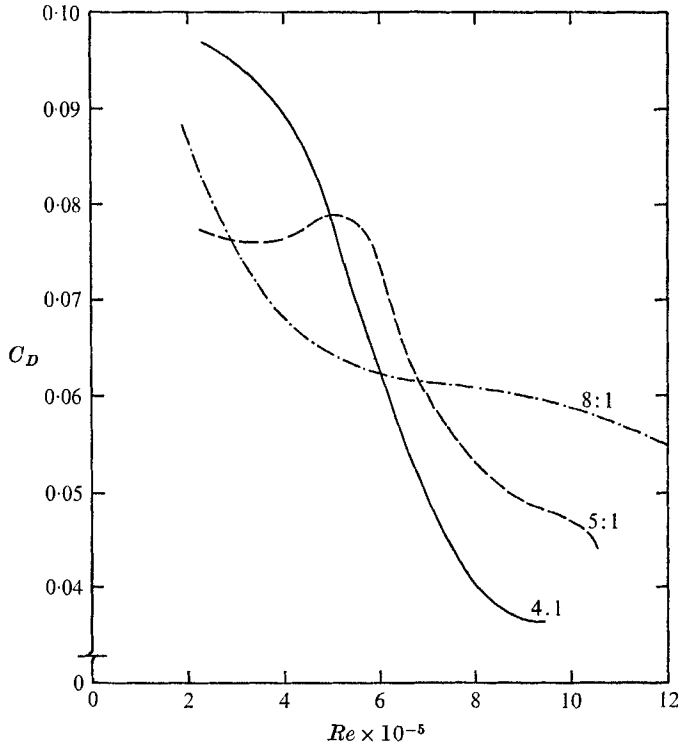

FIGURE 8. C_D versus Re, effect of fineness ratio.

in figure 7 where the effectiveness of the boundary-layer trip is obvious. The qualitative agreement with two-dimensional theory shows that, for the 8:1 ellipsoid at least, large changes in C_D with Reynolds number are associated with transition. Smaller changes would be produced by separation point movement because the pressure drag with these ellipsoids is a small part of the total.

The sensitivity of the measuring technique enabled several small but repeatable peculiarities to be observed with some models. For example, the 5:1 ellipsoid in figure 4(*e*) exhibited a 'hysteresis' loop in that, over part of the speed range, the drag measured with slowly increasing tunnel speed differed from that during a speed reduction. This could perhaps be explained by a transition point lagging in its rearward movement during the speed decrease phase. A completely repeatable irregularity at the upper end of the speed range is shown for the 8:1 ellipsoid in figures 1(*b*) and 6. Detailed investigations were not carried out into these pecularities because they represent small perturbations in C_D and are probably related to individual model shape and surface irregularities.

The effect of fineness ratio for the models with natural boundary-layer transition is shown in figure 8. There appears to be little consistency at the lower Reynolds numbers. At the upper end, the lower the fineness ratio the lower the drag coefficient. This is consistent with other results (Goldstein 1965) which suggest that, at Re greater than 10^6, the L/D ratio for minimum C_D is about 4:1.

5. Concluding remarks

Drag coefficients have been measured in the transition Reynolds number range for a series of ellipsoids having laminar boundary layers or laminar–turbulent transition boundary layers and no support interference.

The effect of fineness ratio is not clear, but supports the suggestion of 4:1 as an optimum ratio at Reynolds numbers greater than 10^6.

This work was sponsored by NASA under contract NAS 1–8658. Mr Harleth Wiley of NASA Langley Research Center was the project monitor.

Appendix A

Wind tunnel turbulence level

Measurement of the test section turbulence level was obtained in Vlajinac (1970) using a constant-current hot-wire anemometer system. The results of these measurements indicate a maximum turbulence level during the present tests to be less than 0·25 % (mean-square fluctuating velocity/mean velocity). This level of turbulence occurred with the largest model tested at a test section free-stream Reynolds number of $1{\cdot}9 \times 10^6$ per foot. At a Reynolds number of $1{\cdot}0 \times 10^6$ per foot the measured turbulence drops to 0·07 %.

A qualitative indication of the turbulence level in the test section can be inferred from the fact that the boundary layer on the walls has a laminar growth rate over the entire 3 foot length of the test section for Reynolds numbers below

$3{\cdot}0 \times 10^6$ per foot. It is therefore concluded that the test section turbulence level during these tests is not sufficiently high to induce abnormally premature transition on the model boundary layers.

Dynamic pressure variation in test section transverse variation

The variation of dynamic pressure across the test section is described in Vlajinac (1970). Measurements were made with a pitot tube rake and the results show that the maximum variation in dynamic pressure is less than 0·2 % of the mean dynamic pressure.

Axial variation

In the axial direction, the dynamic pressure decreases along the test section due to a slight overexpansion of the tunnel walls. This variation in dynamic pressure was measured in Vlajinac (1970) to be 0·063 % per inch. The horizontal buoyancy caused by this axial pressure produces an effective decrease in the measured drag coefficient with a maximum of 0·5 % in the case of the largest model tested. This effect was taken into account in the data presented and was considerably smaller in the case of the other models tested.

Appendix B. Solid blockage corrections

The notation used is that of Pankhurst & Holder (1952). The solid blockage factor ϵ_s is defined by

$$\epsilon_s = U_F/U_T - 1,$$

where U_F is the actual tunnel speed at the model position with the model present and U_T is the tunnel speed indicated by the calibration, i.e. U_T is unaffected by the blockage.

The theoretical prediction of ϵ_s for a solid of revolution is given in Bozorth (1951) as

$$\epsilon_s = \tau\lambda(A/C)^{\frac{3}{2}},$$

where τ is a factor related to tunnel cross-section shape, λ is a factor determined by the model shape, A is the model maximum cross-sectional area and C is the wind tunnel cross-sectional area at the model station. For the octagonal tunnel and 8:1 ellipsoid, the values taken were $\tau = 0{\cdot}77$ and $\lambda = 7{\cdot}5$.

The blockage factor is used to correct the drag coefficient to the free air value C_D by the relationship

$$C_{DF} = C_D/(1+\epsilon_s)^2.$$

REFERENCES

Batchelor, G. K. 1967 *Introduction to Fluid Dynamics*. Cambridge University Press.

Bozorth, R. M. 1951 *Ferromagnetism*. Van Nostrand.

Curle, N. & Skan, S. W. 1957 Approximate methods for predicting separation properties of laminar boundary layers. *Aeron. Quart.* **8**, 257–268.

Durand, W. F. (ed.) 1943 *Aerodynamic Theory*, vol. I, sec. C–VII. Durand Reprinting Committee, Cal Tech.

Goldstein, S. (ed.) 1965 *Modern Developments in Fluid Mechanics*, vol. II. Dover.

JOSEPHS, H. J. & BROOK, V. S. 1953 The probable error of the mean of a small sample. *Dollis Hill, London, Post Office Engineering Department Res. Rep.* no. 13801.

LAMB, H. 1932 *Hydrodynamics.* Cambridge University Press.

PANKHURST, R. C. & HOLDER, D. W. 1952 *Wind Tunnel Technique.* London: Pitman.

ROSENHEAD, L. (ed.) 1963 *Laminar Boundary Layers.* Oxford University Press.

STEPHENS, T. 1969 Construction and preliminary evaluation of prototype magnetic balance and suspension system. *NASA* CR-66903.

VLAJINAC, M. 1970 Design, construction and evaluation of a subsonic wind tunnel. SM Thesis, Massachusetts Institute of Technology.

VLAJINAC, M. & GILLIAM, G. D. 1970 Aerodynamic testing on conical configurations using a magnetic suspension system. *USAF Aerospace Research Laboratory Report* ARL-70-0067, Wright-Patterson Air Force Base, Ohio.